matters

Cell surface expression of integrin β4-subunit in the absence of α6-subunit

Satu-Marja Myllymäki, Aki Manninen

Oulu Center for Cell-Matrix Research, Faculty of Biochemistry and Molecular Medicine, Biocenter Oulu, University of Oulu, Developmental Biology Program, Institute of Biotechnology, University of Helsinki; Oulu Center for Cell-Matrix Research, Faculty of Biochemistry and Molecular Medicine, Biocenter Oulu, University of Oulu

Correspondence
satu-marja.mylly-maki@helsinki.fi
aki.manninen@oulu.fi

Disciplines
Molecular Cell Biology
Biochemistry

Keywords
Hemidesmosome
Basement Membrane
Integrin
Laminin
Epithelial Polarity

Type of Observation
Standalone

Type of Link
Standard Data

Submitted Nov 13, 2018
Published Mar 13, 2019

Triple Blind Peer Review
The handling editor, the reviewers, and the authors are all blinded during the review process.

Full Open Access
Supported by the Velux Foundation, the University of Zurich, and the EPFL School of Life Sciences.

Abstract

Laminin-rich basement membrane (BM) guides epithelial cell polarity, regulates epithelial cell behavior and maintains the integrity of epithelial tissues. αβ1- and α6β4-integrins both contribute to laminin adhesion and signaling via the assembly of integrin adhesion complexes that help to orient the apico-basal polarity axis. β4-integrin differs from other integrin subunits due to its large cytoplasmic domain that connects to cellular intermediate filament (IF) networks in specialized adhesions called hemidesmosomes (HD). β4-integrin is only known to form a heterodimer with the α6-subunit. In normal tissues, β4-integrin is expressed in cells that also express the α6-subunit. However, in most cells analyzed, β4-integrin is expressed in large excess over α6-integrin and in some tumor cells, β4-integrin appears to promote tumorigenic signaling despite loss of HDs formation. The fate of free β4-subunit and its potential functions in cells have not been extensively studied. Here, we have studied subcellular localization and potential surface delivery of β4-integrin in the absence of its heterodimer partner α6. We provide evidence that a significant fraction of β4-subunit can reach the cell surface without α6-subunit. We also report that β4 is cleaved at its extracellular domain to produce a membrane-bound proteolytic product with an intact cytoplasmic domain. The processed β4-integrin did not co-precipitate with α6-subunit. Taken together, our data suggest that β4-integrin might have functions that are independent of heterodimer formation.

Introduction

α6β4-integrin is an epithelial-specific heterodimeric extracellular matrix (ECM) receptor that binds select laminin isoforms of the epithelial basement membrane (BM) and forms the core of hemidesmosomes (HDs) [1] [2]. β4-integrin deviates from other integrins due to its large cytoplasmic domain that is responsible for binding to intermediate filaments (IFs) via plakins [3]. HDs establish mechanically robust connections between the ECM and cellular IF networks [4]. Together with laminin-binding β1-integrins, such as α2β1, α3β1 and α6β1, α6β4-integrins convey signals from the BM to regulate epithelial cell polarity [5] [6]. Although all of these integrins bind to laminin, they are only partially functionally redundant. Integrins have specific signaling roles that are critical to their functions in epithelial cells [7] [8] [9].

The intracellular domain of β4 possesses unique binding properties that are regulated on a different basis compared to other β-integrins subunits. Recent study suggests that α6β4 favors an extended conformation that might render it constitutively signaling competent [10]. It is now understood that the binding properties of the β4-tail are regulated by phosphorylation of the β4-tail in response to growth factor signaling [11]. Studies with chimeric receptors have shown that the cytoplasmic tail of β4 can support HD interactions and engage in signaling in the absence of the extracellular domain, which is required for heterodimerization with α6 [12] [13] [14] [15]. Ligand-binding can also occur in the absence of the intracellular domain interactions [16] [17] [18], suggesting that the intra- and extracellular domains of β4 can indeed be functionally uncoupled. Earlier studies have shown that β4-subunit forms heterodimers only with the α6-subunit, but is detected in excess over the α6-subunit, also at the cell surface [19] [20]. Based on pulse-chase analysis of integrin α6 immunocomplexes, it was assumed that monomeric β4-subunit cannot be translocated to the cell surface and thus the free β4-subunit at the cell surface must derive from the dissociated α6β4-heterodimer. However, as free inte-

grin β4 cannot be expected to co-precipitate with the α6-subunit, these results do not exclude the possibility that β4 integrin can be translocated to the cell surface as a single subunit. Interestingly, Klinowska et al. reported that α6-integrins were not required for early mammary gland development and demonstrated a presence of HD-like adhesions in mammary epithelial cells lacking α6-integrin [21]. In contrast, a more recent study found that β4-integrin expression is essential for mammary gland development [22]. Taken together, these findings suggest that β4-integrin might have functions that are independent of the formation of α6β4-heterodimer.

Objective

Given the possible α6-integrin-independent cellular function of β4-subunit, we have here revisited this topic by studying the expression and localization of β4-integrin in α6-integrin knockout (α6KO) MDCK cells. This study has important implications for the cellular role of β4-integrins because monomeric β4-subunit could potentially be signaling-competent.

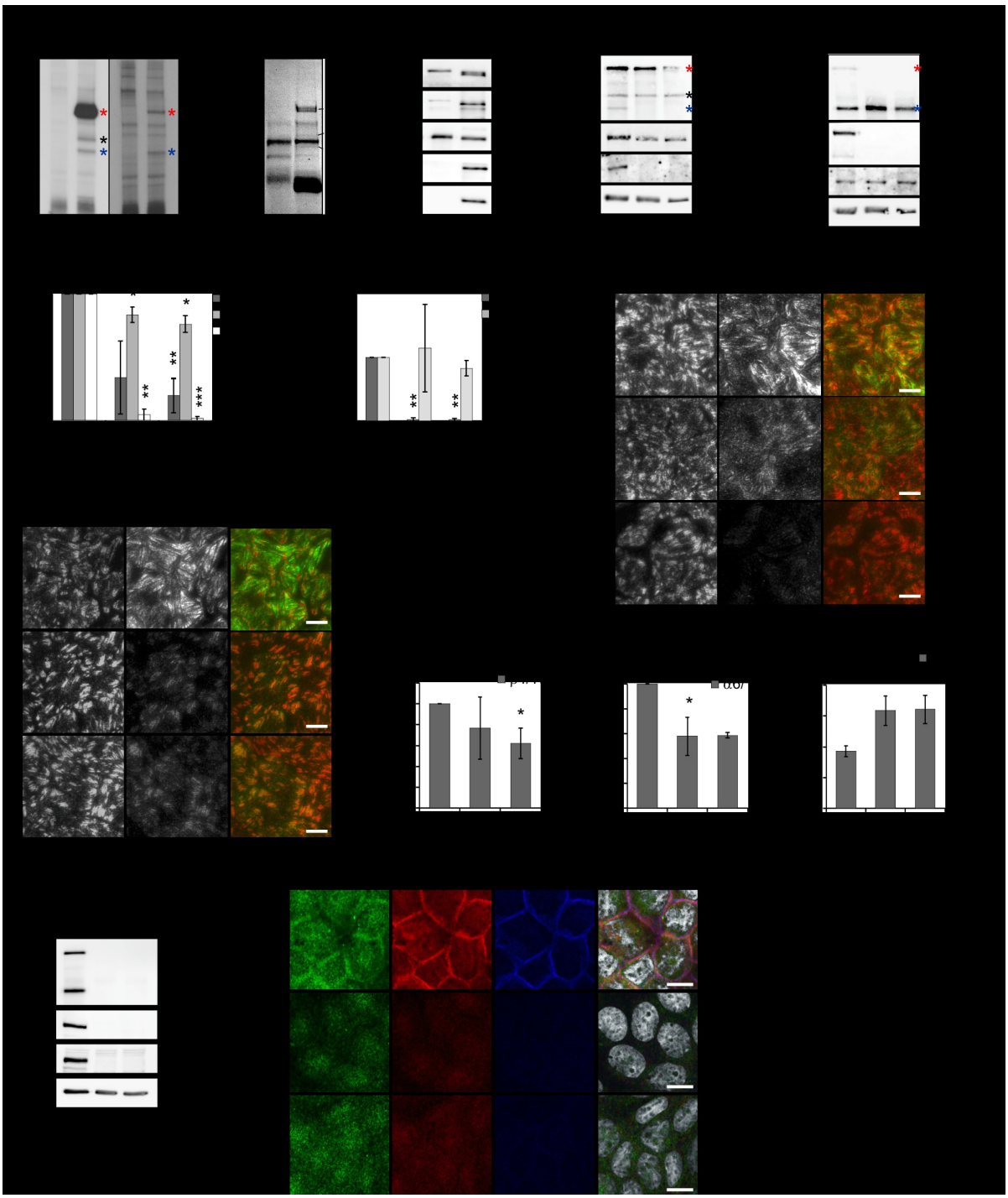

a

Figure Legend

Figure 1. Integrin β4 subunit can reach the cell surface independently of the integrin α6 subunit.

(A) Metabolically labeled proteins co-precipitating with endogenous integrin α6 and β4 in MDCK cells were resolved by SDS-PAGE in reducing conditions and visualized by autoradiography. Non-specific IgG was used for control immunoprecipitations.

(B) Coomassie staining of integrin β4 (β4) and non-specific IgG (IgG) co-precipitating proteins.

(C) Validation of the surface biotinylation method by Western blotting for selected markers for endosomes (EEA1), plasma membrane (Ecad), endoplasmic reticulum (Caln) and cytoplasmic microtubules (β-tub).

(D) Detection of surface expression of integrin β4 subunit in control and α6KO MDCK cells and **(E)** integrin α6 subunit in control and β4KO MDCK cells.

(F-G) Quantification of surface expressed integrins in α6KO **(F)** and β4KO **(G)** cells by densitometry (n=3 experiments).

(H-I) TIRF imaging of talin (red) co-immunostained with integrin β4 (green) in control and α6KO cells **(H)** and with integrin α6 (green) in control and β4KO cells **(I)**.

(J-K) Fluorescence intensity measurements of integrin staining from TIRF images. Intensity ratios were determined relative to talin signal intensity (15–17 images from 3 experiments were analyzed).

(L) TIRF-microscopy based co-localization analysis of integrin α6 and talin in control and β4KO cells was determined by measuring Pearson's correlation coefficients (13 images from 3 experiments were analyzed).

(M) Surface expression levels of α6-integrin in surface biotinylated control and β1/β4-dKO cells were analyzed by streptavidin-HRP blotting of α6-immunoprecipitations. Depletion of β1- and β4-integrins was confirmed by western immunoblotting of whole cell lysate.

(N) Confocal images of co-immunostained β4- (green), α6- (red) and β1-integrins (blue) in control and in the two β1KO cell lines. A confocal slice at the lateral cell membrane is shown.

Statistical significance of fold changes **(F-G & J-K)** was tested with two-tailed one sample t test and PCC values **(L)** with one-way analysis of variance using Tukey's post hoc correction (*p< 0.05, **p< 0.01, ***p< 0.001). Scale bars = 10 μm.

Results & Discussion

To measure the levels of β4-integrin and its heterodimer partner α6-integrin, we first performed steady state metabolic labeling followed by immunoprecipitation with either β4- or α6-integrin antibodies or their respective control IgGs (Fig. 1A). β4-integrin antibodies precipitated a major band at 200 kD (Fig. 1A, left panel, red asterisk) and two additional bands at 150 kD (black asterisk) and 120 kD (blue asterisk). α6-integrin antibodies detected two specific bands at a 1:1 stoichiometric ratio, one at 200 kD (Fig. 1A, right panel, red asterisk) and another at 120 kD (Fig. 1A, right panel, blue asterisk). We have identified these bands in a recent study using mass spectroscopy as full-length β4- (β4-FL) and α6-subunits, respectively (Fig. 1B) [23]. The additional <150 kD fragment, precipitating with an antibody binding to the C-terminus of β4-integrin, was identified as a truncated form of β4-integrin (β4-C) that was lacking most of its extracellular domain. Proteolytic cleavage of β4 from the ectodomain by MMP family of proteases has been reported [24]. To investigate if β4 is similarly processed in MDCK cells by MMPs to release a fragment of the observed size, we treated cells with different concentrations of a broad-spectrum MMP inhibitor. The results indicated that the fragment was indeed sensitive to the inhibitor in a concentration dependent manner, suggesting that β4 ectodomain is generated by MMP-dependent proteolytic cleavage (Fig. S1A). β4-C did not immunoprecipitate with α6-integrin (Fig. 1A). Taking together, these data show that β4 formed a single heterodimer with α6 in MDCK cells. However, as β4-integrin is found in large excess over α6, only a small fraction of total β4 forms a α6β4-heterodimer.

To investigate whether α6β4 integrins are obligate heterodimers or if β4 can mature independently of α6, and vice versa, we generated knockout (KO) cell lines by CRISPR/Cas9-mediated gene editing using a lentivirus-mediated co-expression system for single gRNA constrts and Cas9 [25]. Two independent gRNA constructs were designed for each target gene and puromycin-selected ItgKO cell populations (Fig. S1B)

were screened by western immunoblotting (β4, Fig. S1C) and immunofluorescence (α6, Fig. S1D) for clones that had lost the target protein expression (Fig. S1B). Three verified KO-clones from each construct were selected for further experiments (indicated in Fig. S1C and S1D). Note the disappearance of both β4-FL and β4-C bands in β4KO cells (Fig 1E).

To study the maturation and cell surface targeting of β4-integrin, we performed a surface biotinylation assay in control, β4- and α6KO MDCK cells. Specific biotinylation of cell surface proteins by was confirmed by western blotting of selected cell surface (β4-integrin, E-cadherin) and cytoplasmic (Early endosomal antigen 1 (EEA1), calnexin, β-tubulin) proteins from streptavidin precipitations (Fig. 1C). Strikingly, both β4-FL and particularly the β4-C could be detected at the surface of α6KO cells (Fig. 1D & F). While clones from the α6-KO construct 2 (α6KO2) expressed significantly lower levels of β4-FL at the cell surface compared to α6KO1, all of them retained normal surface levels of β4-C and α6-KO clone 1 (α6KO1) displayed high levels of surface expressed β4-FL. Moreover, α6 was abundantly expressed at the surface of both Itgβ4-KO cell clones (Fig. 1E & G).

To confirm the surface expression with an independent method we employed total internal reflection fluorescence (TIRF) microscopy that limits the excitation depth to roughly 100 nm from the refractive surface thereby detecting only fluorescence signals that are at, or very close to, the basal surface of the cells. The basal localization of α6- and β4-subunits was analyzed in the different KO cell lines. TIRF analysis in control cells revealed a characteristic hemidesmosome-like elongated staining pattern with antibodies recognizing β4- or α6-integrins (Fig. 1H & I, middle panels). These patches were adjacent but distinct from talin (TLN)-positive focal adhesions (Fig. 1H & I, left panels). In agreement with the surface biotinylation data, the α6KO1 exhibited more robust patchy β4-positive signal at the basal membrane than α6KO2 clone, but both of them showed detectable β4-staining (Fig. 1H–K). In β4KO cells, α6-integrin targeting to the basal surface domain was also reduced but, in addition, the remaining α6-staining pattern changed such that it better coincided with talin (Fig. 1I, 1K & L). β1-integrins and TLNs are central components of actin-linked focal adhesions [26] [27]. Because β1-integrin was not visible in the α6-integrin immunoprecipitations, our data suggests that either free α6-subunit can also reach the cell surface or the α6-antibody disrupts α6β1-integrin heterodimers during immunoprecipitation. Given that α6-integrin showed increased co-localization with TLN in β4-KO cells, we next addressed this issue by generating β1/β4-dKO cells lacking expression of both β1- and β4-integrins and studied the surface levels of α6-integrins in these cells (Fig. 1M). This data clearly showed that the surface expression of α6-subunit in β4-KO cells was entirely dependent on heterodimer formation with β1-subunit (Fig. 1M & N). In the absence of β4-subunit, α6-integrin can be secreted to the plasma membrane as α6β1-heterodimer. However, β4-integrin is required for its localization to putative HDs (Fig. 1I & N). Lateral and basal expression of α6β4-integrin was unaffected by depletion of β1-integrin (Fig. S2B).

Our data showed that β4-integrin is able to reach the cell surface in the absence of α6-integrin. The surface expression of α6-subunit was dependent on heterodimer formation with either β4 or β1 (Fig. 1M-N & Fig. S2). Consistent with earlier findings, we found no evidence for a novel β4-subunit containing integrin heterodimer in α6KO cells. This result contrasts the current model according to which β4-integrin would remain trapped in the ER until it forms a heterodimer with α6-integrin. However, it should be noted that previous data supporting an independent HD targeting of both extracellular and intracellular domains of β4-integrins has been reported [12] [15] [18]. Moreover, a previous study detected a significant amount of monomeric β4-integrin at the cell surface, although it was suggested to derive from the α6β4 complex via partial dissociation or due to faster turnover rate of the α6-subunit [20]. Based on current results, a significant amount of free, presumably monomeric, β4-integrin exists at the cell surface also in the absence of α6-subunit expression, suggesting that it can be transported to the cell surface as a single subunit. How stable such monomeric β4-integrin is, remains unknown. The observation that the relative amount of processed β4-integrin (β4-C), lacking almost the entire extracellular domain, was increased in α6KO cells suggests that monomeric β4-integrins might be prone to proteolytic processing after which

they are not able to mediate adhesion to laminin. In line with this finding, mouse studies have shown that α6-deletion leads to loss of functional HDs and results in lethal fragility in epithelial tissues [28]. However, the processed β4-C could still promote partial assembly of HD components and help to link other laminin receptor complexes, such as those mediated by β1-integrins or non-integrin receptors like the dystroglycan, to the IF network. Further studies are warranted to explore these possibilities.

Conclusions

In conclusion, our data shows that free β4-integrin can be targeted to the cell surface where it forms HD-like structures also in the absence of α6-subunit, although with visibly reduced efficiency. The ectodomain of surface expressed β4-integrins can be proteolytically cleaved and this process is enhanced in α6-KO cells. Nevertheless, steady-state biosynthetic labeling experiments confirmed that significant levels of full-length free β4-integrins are expressed at the cell surface. Whether this monomeric β4-integrin is signaling-competent and has independent cellular functions remains to be studied.

Limitations

The current study is based on in vitro cell culture model. Whether β4-integrin can be found at cell surface in, for example, α6-integrin-deficient mice, remains to be studied.

Alternative Explanations

Conjectures

The initial findings should be followed by studies addressing the signaling potential of β4-integrin in α6-deficient cells.

Additional Information

Methods

Antibodies and Reagents

Primary antibodies (see also Table S1) targeting β1-integrin were purchased from Thermo Fischer Scientific (TS2/16; #MA2910). Anti-β4-integrin antibodies were purchased from Santa Cruz (sc-6628) and anti-α6-integrin (555734-GoH3) and anti-E-cadherin (610181) antibodies were from BD Biosciences. Anti-LN-γ1 (L9393), anti-β-actin (A5441), anti-β-tubulin (T4026) and anti-talin (T3287) antibodies were from Sigma-Aldrich. Anti-Calnexin (ab10286) and anti-EEA1 (ab2900) antibodies were from Abcam. Peroxidase-conjugated secondary antibodies for western immunoblotting and fluorophore-conjugated secondary antibodies for immunofluorescence stainings were purchased from Jackson Immunoresearch. Goat and rat total IgGs, used as negative controls in immunoprecipitations, were also from Jackson Immunoresearch. Alexa Fluor 488 phalloidin from Invitrogen was used for staining of F-actin and DAPI from Sigma-Aldrich was used for staining of nuclei. Surface-biotinylated and immunoprecipitated proteins were detected from western immunoblots using peroxidase streptavidin (Jackson Immunoresearch).

Cell culture and Treatments

MDCK-II cells (ATCC:CCL-34) were routinely cultured in 5% fetal bovine serum (Invitrogen) containing minimal essential medium (MEM, Invitrogen) with 1% penicillin and streptomycin. For analysis of matrix adhesions in confluent cells, cells were seeded onto

coverslips or glass bottom dishes (for TIRF microscopy) and cultured in serum containing medium for 6 days. When indicated, cells were cultured in the presence of GM6001 (Sigma-Aldrich) at different concentrations for 24 h.

KO of integrins via lentivirus-mediated expression sgRNAs and Cas9

Gene editing with lentivirus-mediated co-expression of Cas9 and sgRNA-constructs was done with some modifications as previously described [25]. Second exon of canine ITGA6 and fourth exon of canine ITGB4 were used as a template for gRNA-design. Target sequences with no off-target sites with less than 3 mismatches in the canine genome database (European Nucleotide Archive), were selected based on FASTA similarity search tool (EMBL-EBI; Table S2). Two targeting sequences for each gene were selected and the corresponding gRNA oligos with BsmBI overhangs were subcloned into lentiCRISPRv1 (β4- and α6-KOs; Addgene #49535) or lentiCRISPRv2 (β1-KOs; Addgene #52961, [29]).

For generation of the lentiviruses, 70–80% confluent 293T cells on CellBind 10 cm dishes (Corning) were co-transfected with lentiCRISPRv1 (20 µg), pPAX2 (15 µg) and VSVg (5 µg) by Lipofectamine 2000 reagent (Invitrogen) in OptiMEM (Invitrogen). Medium was collected over a period of 24 h to 96 h post-transfection in 12 h patches. Virus-containing medium was pooled and filtered through a 0.44 µm filter, followed by pelleting of the virus by ultracentrifugation at 100,000 × g for 2 h at 4℃. 1/10th dilution of the 100X virus concentrate was used for infection of MDCK cells seeded at 6×104/24-well, 24 h prior. 24 h post-infection, virus-containing media was exchanged with normal media to allow cells to recover. 48 h post-infection, cells were trypsinized and re-seeded in the presence of 6 µg/ml puromycin, followed by 24 h of selection. Puromycin-resistant cells were analyzed for KO frequency using immunofluorescence staining (Fig. S1B). Clonal cell populations were generated and analyzed for loss of protein expression as shown in figure S1C and S1D. Three clonal cell lines for each gRNA construct were generated and used in replicate experiments.

Cell surface biotinylation

Cell surface biotinylation was adapted from [30]. Cells were seeded at a density of 4.5×104/cm² onto 10 cm tissue culture dishes 24 h prior. Cells were washed thrice with biotinylation buffer (20 mM HEPES, 130 mM NaCl, 5 mM KCl, 0.8 mM $MgCl_2$ and 1 mM $CaCl_2$), followed by biotinylation with 0.5 mg/ml Sulfo-NHS-LC-Biotin (Pierce) in biotinylation buffer 30 min on ice with gentle rotation. Cells were washed three times with 10 mM Tris-HCl, 0.15 M NaCl, pH 7.45, followed by lysis with RIPA buffer (10 mM Tris-HCl, 0.15 M NaCl, 0.5% SDS, 1% IGEPAL, 1% sodium deoxycholate) supplemented with protease inhibitors (Roche).

Immunoprecipitation and Avidin-precipitation

RIPA-lysates were rotated 30 min +4℃ with Benzonase nuclease (Novagen) and filtered through a 0.45 µm Spin-X column (Corning). Protein concentration was determined with the bicinchoninic acid assay (Pierce). For analysis of surface biotinylated integrins, lysates with 150 µg total protein were incubated o/n at +4℃ with 3 µg of primary antibodies or control IgGs, and immunoprecipitated with 1.5 mg of Protein-G Dynabeads (Invitrogen) or 30 µl of protein-G agarose beads (Pierce) for 2–3 h +4℃ . Beads were washes thrice with RIPA buffer and once with 10 mM Tris-HCl, pH 6.8. For analysis of metabolically labelled integrins, 200–300 µg of total protein was incubated with 5–7.5 µg of primary antibodies or control IgGs and processed as above. Beads were cooked with 2X Laemmli sample buffer with 2% β-mercaptoethanol 4 min at +97℃. Cell surface biotinylated cell lysates were avidin-precipitated with avidin agarose beads (Pierce).

SDS-PAGE and Western immunoblotting

RIPA-lysates were prepared into 1X Laemmli sample buffer with 1% β-mercaptoethanol and cooked 4 min at +97℃. Proteins were separated in 6% SDS-PAGE and blotted o/n at +4℃ at 20V in with 20% ethanol in 0.025 M Tris 0.192 M Glycine onto a nitrocellulose membrane (Perkin-Elmer). Membranes were reacted with primary antibodies o/n at +4℃, followed by incubation with peroxidase-conjugated secondary antibodies (Jackson

Immunoresearch). Antibody bands were detected with the Lumi-Light chemiluminescence kit (Roche) with the LAS-3000 imager. Protein bands were quantified with the Quantity One software (Biorad) and relative levels of KOs were determined either by directly dividing from control or from a standard curve prepared from serially diluted control.

Metabolic labeling and Autoradiography

Metabolic labeling protocol was adapted from [31]. Briefly, cells were seeded as 4×105/cm onto 6 cm Ø tissue culture dishes and cultured for 3 days followed by 18 h of labeling at +37℃ with 100 µCi of EasyTag™ EXPRE35S35S Protein Labeling Mix (PerkinElmer) in medium containing 1/10th normal concentration of methionine and cysteine. Labelled cells were washed three times with cold PBS and lysed in 1 ml of RIPA buffer on ice. For analysis of metabolically labelled integrins, 200–300 µg of total protein was incubated with 5–7.5 µg of primary antibodies or unspecific IgGs. Immunoprecipitation and SDS-PAGE were performed as described above. Gels were de-stained for 10 min at room temperature (RT) with 45% methanol and 10% acetic acid) and impregnated with Kodak™ ENLIGHTNING™ Rapid Autoradiography Enhancer (PerkinElmer) for 30 min at RT in the dark. Gels were dried and exposed onto BioMax® XAR films (Carestream).

Immunofluorescence

Cells were fixed with 4% PFA in PBS+/+ (PBS with 0.5 mM $MgCl_2$ and 0.9 mM $CaCl_2$) for 15 min at RT. After quenching for 20 min with 0.2 M glycine in PBS, cells were permeabilized with 0.1% TX-100 in PBS for 10 min. All subsequent steps on saponin-permeabilized cells contained 0.02% saponin. Permeabilized cells were blocked with 0.5% BSA in PBS for minimum of 30 min and primary antibodies were prepared in blocking buffer and incubated with cells o/n at +4℃. After 1 h incubation with secondary antibodies at RT, cells were mounted with Immu-Mount (company). When used, DAPI and phalloidin dyes were prepared with secondary antibodies. For staining with PAN-cytokeratin antibody, cells were fixed with 1:1 mixed methanol and acetone at -20℃ and quenching and permeabilization steps omitted.

Microscopy and Image analysis

Cells were seeded onto glass coverslips (for confocal microscopy) or glass-bottom dishes (for TIRF) and cultured to confluency. For immunofluorescence staining, cells were fixed with 4% PFA in PBS+/+ (PBS with 0.5 mM $MgCl_2$ and 0.9 mM $CaCl_2$) for 15 min at RT. After quenching for 20 min with 0.2 M glycine in PBS, cells were permeabilized with 0.1% TX-100 in PBS for 10 min. Permeabilized cells were blocked with 0.5% BSA in PBS for minimum of 30 min and primary antibodies, were prepared in blocking buffer and incubated with cells overnight at +4℃. After 1 h incubation with secondary antibodies at RT, cells were mounted with Immu-MountTM (Thermo Fisher Scientific). When used, DAPI and phalloidin dyes were prepared with secondary antibodies. Confocal images were acquired with the Zeiss LSM-780 laser scanning confocal microscope using 40X Plan-Apochromat objective (N.A = 1.4) and TIRF images with the Zeiss Cell Observer spinning disc confocal microscope using the alpha Plan-Apochromat 63X oil objective with an N.A of 1.46. For TIRF image acquisition, immunofluorescence stained samples in glass bottom dishes were left unmounted and were kept in PBS. Co-localization in TIRF images was assessed with the Pearson's correlation coefficient measured with the Co-localization Threshold plugin in FIJI using Costes method auto threshold determination and excluding zero intensity pixels. Unthresholded PCC values were used in the analysis due to the high labelling density of the matrix staining, which interferes with the thresholding algorithm. One channel was rotated 90° degrees relative to the other channel and the misaligned images analyzed to demonstrate the absence of random correlation.

Statistics

Absolute values were tested for significant differences with one-way analysis of variance (ANOVA) using Tukey's post-hoc test. Fold changes were tested for significant

differences with two-tailed one-sample t-test. All statistical analyses were carried out with SPSSv20.

Funding Statement

This work was funded by Academy of Finland (251314, 135560, 263770, and 140974 /AM).

Acknowledgements

Riitta Jokela is acknowledged for overall expert technical assistance. Karl Matlin PhD, Jose Moyano PhD and Patricia Greciano PhD are acknowledged for instructions on immunoprecipitation and radiolabeling techniques. We acknowledge the help from Jaana Träskelin at Biocenter Oulu (BCO) Virus Core Facility laboratory and Veli-Pekka Ronkainen at BCO tissue imaging center.

Ethics Statement

Not applicable

Citations

[1] José M. de Pereda et al. “Advances and perspectives of the architecture of hemidesmosomes: Lessons from structural biology”. In: *Cell Adhesion & Migration* 3.4 (2009), pp. 361–364. DOI: 10.4161/cam.3.4.9525. URL: https://doi.org/10.4161/cam.3.4.9525.

[2] Ryoko Nishiuchi et al. “Ligand-binding specificities of laminin-binding integrins: A comprehensive survey of laminin–integrin interactions using recombinant α3β1, α6β1, α7β1 and α6β4 integrins”. In: *Matrix Biology* 25.3 (2006), pp. 189–197. DOI: 10.1016/j.matbio.2005.12.001. URL: https://doi.org/10.1016/j.matbio.2005.12.001.

[3] Sandy H.M. Litjens, José M. de Pereda, and Arnoud Sonnenberg. “Current insights into the formation and breakdown of hemidesmosomes”. In: *Trends in Cell Biology* 16.7 (2006), pp. 376–383. DOI: 10.1016/j.tcb.2006.05.004. URL: https://doi.org/10.1016/j.tcb.2006.05.004.

[4] Sara A. Wickström, Korana Radovanac, and Reinhard Fässler. “Genetic Analyses of Integrin Signaling”. In: *Cold Spring Harbor Perspectives in Biology* 3.2 (2010), a005116–a005116. DOI: 10.1101/cshperspect.a005116. URL: https://doi.org/10.1101/cshperspect.a005116.

[5] Jessica L. Lee and Charles H. Streuli. “Integrins and epithelial cell polarity”. In: *Journal of Cell Science* 127.15 (2014), pp. 3217–3225. DOI: 10.1242/jcs.146142. URL: https://doi.org/10.1242/jcs.146142.

[6] Aki Manninen. “Epithelial polarity – Generating and integrating signals from the ECM with integrins”. In: *Experimental Cell Research* 334.2 (2015), pp. 337–349. DOI: 10.1016/j.yexcr.2015.01.003. URL: https://doi.org/10.1016/j.yexcr.2015.01.003.

[7] A. R. Howlett et al. “Cellular growth and survival are mediated by beta 1 integrins in normal human breast epithelium but not in breast carcinoma”. In: *Journal of Cell Science* 108.5 (1995), pp. 1945–1957.

[8] Satu Marja Myllymäki, Terhi Piritta Teräväinen, and Aki Manninen. “Two Distinct Integrin-Mediated Mechanisms Contribute to Apical Lumen Formation in Epithelial Cells”. In: *PLOS ONE* 6.5 (2011), e19453. DOI: 10.1371/journal.pone.0019453. URL: https://doi.org/10.1371/journal.pone.0019453.

[9] Valerie M. Weaver et al. “β4 integrin-dependent formation of polarized three-dimensional architecture confers resistance to apoptosis in normal and malignant mammary epithelium”. In: *Cancer Cell* 2.3 (2002), pp. 205–216. DOI: 10.1016/s1535-6108(02)00125-3. URL: https://doi.org/10.1016/s1535-6108(02)00125-3.

[10] Naoyuki Miyazaki, Kenji Iwasaki, and Junichi Takagi. “A systematic survey of conformational states in β1 and β4 integrins using negative-stain electron microscopy”. In: *Journal of Cell Science* 131.10 (2018), jcs216754. DOI: 10.1242/jcs.216754. URL: https://doi.org/10.1242/jcs.216754.

[11] Coert Margadant et al. “Regulation of hemidesmosome disassembly by growth factor receptors”. In: *Current Opinion in Cell Biology* 20.5 (2008), pp. 589–596. DOI: 10.1016/j.ceb.2008.05.001. URL: https://doi.org/10.1016/j.ceb.2008.05.001.

[12] Cecile A. W. Geuijen and Arnoud Sonnenberg. “Dynamics of the α6β4 Integrin in Keratinocytes”. In: *Molecular Biology of the Cell* 13.11 (2002), pp. 3845–3858. DOI: 10.1091/mbc.02-01-0601. URL: https://doi.org/10.1091/mbc.02-01-0601.

[13] Keith D. Merdek et al. “Intrinsic Signaling Functions of the β4 Integrin Intracellular Domain”. In: *Journal of Biological Chemistry* 282.41 (2007), pp. 30322–30330. DOI: 10.1074/jbc.m703156200. URL: https://doi.org/10.1074/jbc.m703156200.

[14] Mirjam G. Nievers et al. “Formation of hemidesmosome-like structures in the absence of ligand binding by the α6β4 integrin requires binding of HD1/plectin to the cytoplasmic domain of the β4 integrin subunit”. In: *Journal of Cell Science* 113.6 (2000), pp. 963–973.

[15] Mirjam G. Nievers et al. “Ligand-independent role of the β4 integrin subunit in the formation ofhemidesmosomes”. In: *Journal of Cell Science* 111.12 (1998), pp. 1659–1672.

[16] Dirk Geerts et al. “Binding of Integrin α6β4 to Plectin Prevents Plectin Association with F-Actin but Does Not Interfere with Intermediate Filament Binding”. In: *The Journal of Cell Biology* 147.2 (1999), pp. 417–434. DOI: 10.1083/jcb.147.2.417. URL: https://doi.org/10.1083/jcb.147.2.417.

[17] Jan Koster et al. “Two Different Mutations in the Cytoplasmic Domain of the Integrin β4 Subunit in Nonlethal Forms of Epidermolysis Bullosa Prevent Interaction of β4 with Plectin”. In: *Journal of Investigative Dermatology* 117.6 (2001), pp. 1405–1411. DOI: 10.1046/j.0022-202x.2001.01567.x. URL: https://doi.org/10.1046/j.0022-202x.2001.01567.x.

[18] L. Spinardi et al. “A recombinant tail-less integrin beta 4 subunit disrupts hemidesmosomes, but does not suppress alpha 6 beta 4-mediated cell adhesion to laminins”. In: *The Journal of Cell Biology* 129.2 (1995), pp. 473–487. DOI: 10.1083/jcb.129.2.473. URL: https://doi.org/10.1083/jcb.129.2.473.

[19] A. Sonnenberg et al. “Identification and characterization of a novel antigen complex on mouse mammary tumor cells using a monoclonal antibody against platelet glycoprotein Ic.” In: *Journal of Biological Chemistry* 263 (1988), pp. 14030–14038.

[20] A. Sonnenberg et al. “The α6β1 (VLA-6) and α6β4 protein complexes: tissue distribution and biochemical properties.” In: *Journal of Cell Science* 96 (1990), pp. 207–217.

[21] Teresa C.M. Klinowska et al. “Epithelial Development and Differentiation in the Mammary Gland Is Not Dependent on α3 or α6 Integrin Subunits”. In: *Developmental Biology* 233.2 (2001), pp. 449–467. DOI: 10.1006/dbio.2001.0204. URL: https://doi.org/10.1006/dbio.2001.0204.

[22] Jiarong Li et al. “Integrin β4 regulation of PTHrP underlies its contribution to mammary gland development”. In: *Developmental Biology* 407.2 (2015), pp. 313–320. DOI: 10.1016/j.ydbio.2015.09.015. URL: https://doi.org/10.1016/j.ydbio.2015.09.015.

[23] Satu-Marja Myllymäki et al. “Assembly of the β4-Integrin Interactome Based on Proximal Biotinylation in the Presence and Absence of Heterodimerization”. In: *Molecular & Cellular Proteomics* 18.2 (2018), pp. 277–293. DOI: 10.1074/mcp.ra118.001095. URL: https://doi.org/10.1074/mcp.ra118.001095.

[24] Sonali Pal-Ghosh et al. “MMP9 cleavage of the β4 integrin ectodomain leads to recurrent epithelial erosions in mice”. In: *Journal of Cell Science* 124.15 (2011), pp. 2666–2675. DOI: 10.1242/jcs.085480. URL: https://doi.org/10.1242/jcs.085480.

[25] Ophir Shalem et al. “Genome-Scale CRISPR-Cas9 Knockout Screening in Human Cells”. In: *Science* 343.6166 (2014), pp. 84–87. DOI: 10.1126/science.1247005. URL: https://doi.org/10.1126/science.1247005.

[26] Benjamin Klapholz and Nicholas H. Brown. “Talin – the master of integrin adhesions”. In: *Journal of Cell Science* 130.15 (2017), pp. 2435–2446. DOI: 10.1242/jcs.190991. URL: https://doi.org/10.1242/jcs.190991.

[27] Aki Manninen and Markku Varjosalo. “A proteomics view on integrin-mediated adhesions”. In: *Proteomics* 17.3-4 (2016), p. 1600022. DOI: 10.1002/pmic.201600022. URL: https://doi.org/10.1002/pmic.201600022.

[28] Elisabeth Georges-Labouesse et al. “Absence of integrin α6 leads to epidermolysis bullosa and neonatal death in mice”. In: *Nature Genetics* 13.3 (1996), pp. 370–373. DOI: 10.1038/ng0796-370. URL: https://doi.org/10.1038/ng0796-370.

[29] Neville E Sanjana, Ophir Shalem, and Feng Zhang. “Improved vectors and genome-wide libraries for CRISPR screening”. In: *Nature Methods* 11.8 (2014), pp. 783–784. DOI: 10.1038/nmeth.3047. URL: https://doi.org/10.1038/nmeth.3047.

[30] Tracy L. Davis et al. “Identification of a Novel Structural Variant of the α6 Integrin”. In: *Journal of Biological Chemistry* 276.28 (2001), pp. 26099–26106. DOI: 10.1074/jbc.m102811200. URL: https://doi.org/10.1074/jbc.m102811200.

[31] Terhi P. Teräväinen et al. “αV-Integrins Are Required for Mechanotransduction in MDCK Epithelial Cells”. In: *PLOS ONE* 8.8 (2013), e71485. DOI: 10.1371/journal.pone.0071485. URL: https://doi.org/10.1371/journal.pone.0071485.